Published in final edited form as:
Exp Brain Res. 2012 October ; 222(3): 277–290. doi:10.1007/s00221-012-3215-4.

Multi-digit coordination during lifting a horizontally oriented object: synergies control with referent configurations

Yen-Hsun Wu, **Vladimir M. Zatsiorsky**, and **Mark L. Latash**
Department of Kinesiology, The Pennsylvania State University, Rec.Hall-267, University Park, PA 16802, USA

Abstract

We explored digit coordination during the acceleration phase of a quick lifting movement of a hand-held horizontal object. We tested three hypotheses related to: (1) the scaling of mechanical variables produced by the hand with changes in the external load, torque, and moment of inertia; (2) changes in the safety margin for the thumb with both the loading conditions and acceleration; and (3) changes in the indices of synergies. The subjects held a horizontal handle with a prismatic grasp (the thumb acted on top of the handle) and performed series of "very quick" lifting movements to a visual target. Multi-digit synergies were quantified as co-variation indices among elemental variables (forces and moments produced by individual digits). The resultant force scaled with the external load but not torque, while the grip force scaled with the external torque but not load. The safety margin dropped with an increase in acceleration; it also showed changes with the external torque and moment of inertia. Total moment of force was primarily produced by the tangential forces (over 80 %) across all movement phases and loading conditions. The index and little fingers produced close to zero moment with their normal forces, while the middle and ring fingers produced consistent moments due to the reproducible shifts of their centers of pressure. Synergy indices at the upper level of the assumed hierarchy (the task is shared between the thumb and virtual finger—an imagined digit with the action equal to that of the four fingers combined) did not drop with acceleration for the three force vector components and one of the moment vector components. They did drop with acceleration at the lower level (virtual finger action is shared among the four fingers). There was a trade-off between synergy indices computed at the two levels for the three force vector components, but not for the moment of force components. We confirmed specialization of different fingers with respect to different task components in quick manipulation tasks. The findings have implications for hypotheses on the control of voluntary movements involving redundant sets of effectors. Within the referent configuration hypothesis, components of a referent configuration may be adjusted to task mechanical characteristics using simple scaling rules. The neural organization of multi-digit synergies in a hierarchal system is able to selectively protect synergies related to stabilization of some performance variables from detrimental effects of the rate of change of those variables. A large number of apparently redundant elemental variables are not the source of additional computational problems but may be beneficial, allowing the central nervous system to facilitate synergies at both levels of the hierarchy.

Keywords

Prehension; Hand; Synergy; Safety margin

Correspondence to: Mark L. Latash.
mll11@psu.edu.

Introduction

One of the main functions of the human hand is to manipulate objects. Commonly, it is necessary to keep orientation of the object constant during the action, for example when moving a mug filled with coffee. This is not a trivial task because hand-held objects differ in their mass and center of mass location. At the level of mechanical analysis, such tasks may be viewed as associated with two subtasks: (1) applying manipulation forces that produce the required action and (2) applying time-varying forces that balance the motion-dependent changes in the external torques to prevent changes in the object orientation.

Most earlier studies addressed manipulation of objects oriented vertically grasped using either a prismatic or a tripod grasp (Burstedt et al. 1999; Baud-Bovy and Soechting 2001; Gentilucci et al. 2003; Shim et al. 2005); only a few considered manipulation of objects with different orientations (Pataky et al. 2004; Gao et al. 2005; Zatsiorsky et al. 2005). Recently, we have described major differences in the coordination of digits during static tasks while holding a horizontally oriented handle with a prismatic grip against various external loads and torques (Wu et al. 2012). This study continues exploration of how humans manipulate such objects.

Lifting a hand-held object in the vertical direction requires coordinated rotations in arm joints. While the desired object motion in the external space may be translational, the associated joint rotations raise a question: Which of the following three time-varying external variables define characteristics of the mechanical action: external load, torque, or object's moment of inertia? We hypothesized (Hypothesis-1) that resultant force and resultant moment of force would scale with corresponding external variables, load and torque. It is harder to make predictions with respect to variables that are not explicitly prescribed by the task such as grip force (internal force applied normal to the object surface), safety margin (proportion of the normal force above the minimal level required to avoid slippage), and indices of co-variation among elemental variables (synergy indices). It should be noted that many studies have explicitly stated or implicitly assumed that keeping the safety margin constant is a priority of the central nervous system that defines the coupling between the normal and tangential forces (cf. Johansson and Westling 1988; Burstedt et al. 1999; Cole et al. 1999; Flanagan et al. 1999; De Freitas et al. 2009). The idea of signal-dependent noise (Harris and Wolpert 1988) suggests that during the acceleration phase of a fast movement, variance of the tangential force increases with its magnitude. So, our Hypothesis-2 was that the safety margin would increase during object acceleration to ensure comparable safety.

When all five digits produce forces on the object, for example, as in the prismatic grasp, the number of constraints associated with typical tasks is smaller than the number of mechanical variables produced by the digits, three force components, and three moment components per digit (elemental variables). We assume that patterns of elemental variables reflect a strategy of uniting these variables into groups with co-variation among the variables within a group that helps reduce variance of (stabilize) their combined output. This assumption follows the principle of abundance (Gelfand and Latash 1998; Latash 2012)—a particular way of dealing with apparent problems of motor redundancy (Bernstein 1967). Co-variation patterns among elemental variables have been addressed as prehension synergies (Zatsiorsky and Latash 2008). As in many earlier studies, we assume that the control of the human hand may be viewed as based on a two-level hierarchy (Arbib et al. 1985; Latash and Zatsiorsky 2009): At the upper level (VF–TH level), the task is shared between the thumb and the virtual finger (VF, an imagined finger with the mechanical action equal to that of the four fingers combined), while at the lower level (IF level), the VF action is shared among the individual fingers.

Several earlier studies reported a drop in the synergy index (index of co-variation of elemental variables) with an increase in the rate of change of the performance variable for which the index was computed (Latash et al. 2002; Goodman et al. 2005; Friedman et al. 2009; Skm et al. 2010). In this study, we explored whether natural changes in the rate of different variables associated with the lifting action are related to a drop in the synergy indices computed for those variables at the VF–TH and IF levels. Several reports of a trade-off between synergy indices at the upper (VF–TH) and lower (IF) levels suggest that a drop in a synergy index at one of the levels may be associated with an increase in the corresponding synergy index at the other level (Gorniak et al. 2007, 2009). It should be noted that performance variables produced by the hand and by the VF separately show parallel changes in their rates of change during a quick lifting action. Hence, our Hypothesis-3 is that some of the synergy indices may not show a drop during the increase in the rate of the corresponding performance variable.

Methods

The current study used the same methods and subjects as the earlier study of static prehension (Wu et al. 2012). Hence, here, we present only a brief description of the methods.

Subjects

Nine right-handed healthy subjects, 27 ± 1.1 years of age (7 males and 2 females), were recruited. None of the subjects had a history of long-term involvement in hand or finger activities such as playing musical instruments. All subjects gave informed consent according to the procedures approved by the Office for Research Protections of the Pennsylvania State University.

Apparatus

Subjects held a handle (total mass was 0.35 kg, Fig. 1a) instrumented with force sensors (model Nano 17-R; ATI Industrial Automation, Apex, NC, USA), and an electromagnetic tracking device (Polhemus LIBERTY, Colchester, VT, USA). Weights could be attached to the handle to create external loads and torques. The local coordinate (x, y, and z) of each sensor was parallel to the global coordinate (X, Y, and Z), Fig. 1b. All sensor centers were in the same plane, the grasp plane, and the grip width (along z-axis) was 6.25 cm. The center of the thumb sensor was aligned with the mid-point between the middle and ring fingers sensors on the opposite side of the handle. All contact surfaces were covered with sandpaper (320 grit) to provide extra friction.

A computer with a 19″ monitor and customized software (LabVIEW 9.0, National Instruments, Austin, TX, USA) was used to collect data and to render visual feedback on the handle orientation. All measurements from the force sensors were collected via a 16-bit data acquisition card (NI PCI-6225, National Instruments, Austin, TX, USA) installed in the computer. The measurements of the tracking device were taken using a USB 2.0 interface. The sampling rate was 100 Hz for all signals.

Procedure

The subject sat in front of the monitor with the upper arm naturally hanging down and the forearm parallel to the ground and the hand supine and pointing forward. The subject was then instructed to lower the wrist to a position about 20 cm below the previous posture with a combined wrist and elbow extension motion. Data collection began after the subject reported that he/she was comfortably holding the handle as instructed. In all trials, the subject held the handle for 3 s (static-hold phase) under the instruction to maintain its

orientation horizontal. The visual feedback on the computer screen showed the orientation of the handle. After 3 s, a sound signal was given and the subject lifted the handle in a self-paced manner to a target 20 cm above the initial position with an elbow flexion movement "as quickly as possible." Once reaching the target height, the subject held the handle statically until the end of the trial. The trial duration was 6 s. After the data collection stopped, the experimenter held the handle and the subject had a 20-s rest interval. There were also 5-min breaks between conditions. The order of conditions was pseudorandomized, and the total duration of the experiment was about 1.5 h.

The experimental conditions were designed to compare the effects of mass, external torque, and the rotational moment of inertia (denoted as I). The conditions were I_{M1L1}, I_{M1L2}, I_{M1L3}, I_{M2L2}, I_{M3L1} = [0.014, 0.021, 0.027, 0.033, 0.064] Nm^2 with respect to the Y-axis of the handle, where the subscripts denote, respectively, the object mass (three levels: $M1$, $M2$, and $M3$ = 0.1, 0.2, and 0.3 kg) and the distance from the center of the handle to the load (three levels: $L1$, $L2$, and $L3$ = 0.08, 0.16, and 0.24 m). The moment of inertia was estimated with respect to the geometrical center of the handle along the global Y-axis. We selected only five mass–distance combinations to minimize fatigue and to have an opportunity to compare conditions with the same mass and different torques ($M1L1$, $M1L2$, and $M1L3$) and with the same torque and different masses ($M1L3$ and $M3L1$). Twenty trials were performed in a single block for each of the five conditions.

Data processing

The data were processed off-line using customized Lab-View software (National Instrument, Austin, TX, USA). All force and position data were low-pass filtered at 30 Hz with the second-order, zero-lag Butterworth filter before further processing. The time derivatives of the resultant vertical force (the resultant normal force acting on the handle, F^n_{RES}) and of the vertical displacement were further low-pass filtered at 5 Hz.

All force and position data were time aligned to the lifting onset (T_0) defined as the instant when the derivative of F^n_{RES} reached 5 % of its maximum peak value in that particular trial. Further, the time of peak F^n_{RES} during the movement was defined (T_{MAX}), as well as the half-time (T_{HT}) between T_0 and T_{MAX}. Movement time (MT) was defined as the period between lifting onset and termination. The time of movement termination was determined as the time when the vertical velocity of the handle dropped to 5 % of the maximum vertical velocity in that particular trial.

All force and position data were measured at three times, T_0, T_{HT}, and T_{MAX}. Based on the small deviations of the handle from the original orientation (presented in "Results," Table 1), we assumed that the handle remained horizontal at least until T_{MAX}. The center of pressure (COP) coordinates for individual digits with respect to the center of the handle were computed as $\left[\mathrm{COP}^X_j;\mathrm{COP}^Y_j\right]=\left[-m^Y_j/F^Z_j;Y_j+m^X_j/F^Z_j\right]$, where m is a local moment of force measured by the sensor, F is the digit force, Y is the global Y-coordinate of each sensor, X and Y indicate global coordinates, and subscript j denotes digits (j = {TH, I, M, R, and L} referring to the thumb, index, middle, ring, and little fingers, respectively). Six constraints of the forces applied on the handle at any given time before T_{MAX} were as follows:

$$
\begin{aligned}
F^X_{\text{net}} &= \sum_j \left[F^{t,X}_j\right] = 0 \\
F^Y_{\text{net}} &= \sum_j \left[F^{t,Y}_j\right] = 0 \\
F^Z_{\text{net}} &= \sum_j \left[F^{t,Z}_j\right] + w = 0 \\
M^X_{\text{net}} &= \sum_j \left[M^{t,Y}_j + M^n_j\right] \\
&= \sum_j \left[F^{t,Y}_j \times d_j + F^n_j \times \text{COP}^Y_j\right] = 0 \\
M^Y_{\text{net}} &= \sum_j \left[M^{t,X}_j + M^n_j\right] + T \\
&= \sum_j \left[F^{t,X}_j \times d_j + F^n_j \times \text{COP}^X_j\right] + T = 0 \\
M^Z_{\text{net}} &= \sum_j \left[M^{t,X}_j + M^{t,Y}_j\right] + \sum_j \left[m^Z_j\right] \\
&= \sum_j \left[F^{t,Y}_j \times \text{COP}^X_j - F^{t,X}_j \times \text{COP}^Y_j\right] + \sum_j \left[m^Z_j\right] = 0
\end{aligned}
$$

where j = {TH, *I, M, R,* and *L*}; w is the total weight of the object; T is the external torque; m is a local moment of force; M is moment of force and F is digit force; d is the distance along Z-axis from the center of the handle to the contact surface of a sensor; subscripts *X, Y,* and Z show the direction of a vector; superscripts t and n denote tangential and normal forces.

The resultant normal force (F^n_{RES}) was calculated as $\sum_j \left[F^n_j\right]$. The total moment of force about the Y-axis (M^Y) was $\sum_j \left[M^{t,X}_j + M^n_j\right]$. The grip force ($F_{\text{GRIP}}$) was estimated as the sum of the absolute magnitude of all digit forces in Z direction minus the F^n_{RES}. Sharing of M^Y was computed as $S_j(i) = \left[M^i_j / M^Y\right] \times 100\%$, where j = {TH, *I, M, R,* and *L*}, i denotes the direction of force inducing the moment ($i = n$ or t).

The mechanical effects of the virtual finger (VF) were computed as the summed-up mechanical effects of the four fingers (*I, M, R,* and *L*), that is, $F^i_{VF} = \sum_j \left[F^i_j\right]$, $M^i_{VF} = \sum_j \left[M^i_j\right]$ where i = {*X, Y,* and *Z*}, and j = {*I, M, R,* and *L*}. The VF center of pressure (COP_{VF}) was calculated as: $\left[\text{COP}^X_{\text{VF}}, \text{COP}^Y_{\text{VF}}\right] = \left[-\left(M^Y_{\text{VF}} + d \times F^X_{\text{VF}}\right)/F^Z_{\text{VF}}, \left(M^X_{\text{VF}} - d \times F^Y_{\text{VF}}\right)/F^Z_{\text{VF}}\right]$, where d is the lever arm equal to the half of the grip width.

The safety margin (SM) was defined as: $\text{SM} = \left[|F^n| - \frac{|F^t|}{\mu_s}\right]/|F^n|$, where μ_s is the coefficient of static friction between the fingertip and the grasping surface (defined as a function of normal force, see Wu et al. 2012).

Multi-digit synergies were quantified as the co-variation (across trials) among elemental variables (EV) produced by each digit. The index of synergies was computed as:

$$\Delta V = \left[\sum \text{Var}(\text{EV}) - \text{Var}\left(\sum \text{EV}\right)\right] / \sum \text{Var}(\text{EV})$$

At the VF–TH level, EVs were the variables produced by the VF and TH. At the IF level, the variables produced by individual fingers within the VF were EVs. It should be noted that $\Delta V_{\text{VF–TH}}$ ranges from –1 to 1, and ΔV_{IF} ranges from –3 to 1. Before statistical parametric

analyses, ΔVs were subjected to the modified Fisher's *z*-transform,

$\Delta V_Z = 0.5 \quad \ln\left[\frac{|B_L|+\Delta V}{B_U-\Delta V}\right] - 0.5 \quad \ln\left[\frac{|B_L|}{B_U}\right]$, where B_L is the lower limit and B_U is the upper limit of ΔV.

Statistics

The descriptive statistics are presented as means and standard errors in the text and figures. Repeated measures analyses of variance (rANOVAs) and multivariate analyses of variance (MANOVAs) were performed using SPSS software (SPSS 19, IBM, Somers, NY, USA). One-way repeated measures ANOVAs were conducted on the MT, T_{MAX} with the factor *MOI* (moment of inertia: five levels).

We investigated the effects of mass, torque, and MOI on the variables (F^n_{RES}, M^Y, F_{GRIP}, and SM) across the three phases (T_0, T_{HT}, and T_{MAX}). Because of the limited set of experimental conditions, four different analyses were performed across subsets of conditions. Two-way ANOVAs *Phase* (three levels) × *MOI* (five levels) were conducted to check the overall effects of movement phases and moment of inertia on F^n_{RES}, M^Y, F_{GRIP}, and SM_Z (Fisher-transformed SM). Two-way ANOVAs *Phase* (three levels) × *Torque* (three levels) were used to identify the effects of phases and torques on the same four variables across the low mass conditions (M_1L_1, M_1L_2, and M_1L_3). Finally, two-way ANOVAs *Phase* (three levels) × *Mass* (two levels) were used to check the effects of mass across two torque levels: M_2L_1 versus M_1L_2; and M_3L_1 versus M_1L_3.

A two-way MANOVA was performed on the *COP* in anterio-posterior direction (COP_X), and two MANOVAs Phase (three levels) × *MOI* (five levels) were performed on ΔV_Z.

Results

General characteristics of the action

Across conditions and subjects, the average movement time (MT) was 694 ± 14 ms and the average time to peak resultant normal force (T_{MAX}) was 175 ± 5 ms. While the lifting motion was unconstrained, all subjects performed the task consistently across conditions, with relatively minor deviations of the handle orientation and minor translations along the non-vertical directions. Averaged across subjects' rotational and translational deviations of the handle from the steady state are presented in Table 1 for T_{MAX} and half of that time from movement initiation (T_{HT}). Note the small values of all the variables.

Figure 2 illustrates typical time series for a subset of tasks for a representative subject. The resultant normal force (F^n_{RES}, a) and moment of force about the *Y*-axis (M^Y, c) show similar time profiles with two peaks corresponding to the acceleration and deceleration phases. The grip force (F_{GRIP}, b)—estimated as the sum of the absolute magnitudes of all the digit normal forces minus F^n_{RES}—shows a single peak. Two of the conditions correspond to the same mass and different external torques (M_1L_1 and M_1L_3), while another pair illustrates the patterns for different masses and the same torque (M_1L_3 and M_3L_1). Note the similar trajectories along the vertical axes under different conditions (Fig. 2d; see also Fig. 3d).

Figure 3 presents the same variables averaged across subjects with standard error shades. The figure suggests that F^n_{RES} was affected by mass but not torque, while both F_{GRIP} and resultant M^Y showed strong effects of torque but not mass.

Scaling of the main mechanical variables

Three mechanical variables (F^n_{RES}, F_{GRIP}, and M^Y) were quantified at three phases of the movement, action initiation (T_0), half-time to peak F^n_{RES} (T_{HT}), and time of peak F^n_{RES} (T_{MAX}). Three of the five experiment conditions have been selected to illustrate the main results in the following figures: M_1L_1, M_1L_3, and M_3L_1. To remind, $M1$ = 0.1 kg, $M3$ = 0.3 kg, $L1$ = 0.08 cm, and $L3$ = 0.024 cm (see "Methods"). Hence, comparisons between M_1L_1 and M_1L_3 allow testing effects of changes in the torque, while mass is kept constant. Comparisons between M_1L_1 and M_3L_1 allow testing effects of changes in mass, while torque is kept constant.

Figure 4a shows that F^n_{RES} increased during the lifting phases with mass (different values for M_1L_1 and M_3L_1) but not with torque (similar values in M_1L_1 and M_1L_3). Note that the limited set of masses and lever arms in the study did not allow using a single ANOVA to analyze the effects of mass, torque, and moment of inertia (MOI). Hence, we used two-way repeated measures ANOVAs on F^n_{RES} across subsets of conditions. The ANOVAs explored the effects of MOI, mass, and torque across the three phases (for details see "Methods"). F^n_{RES} increased during the acceleration phase (main effect of *Phase*: $F_{(2, 16)} > 46.965$, $p < 0.01$); it was higher for conditions with higher mass (main effect of *Mass*: $F_{(1, 8)} > 84.568$, $p < 0.01$) and for conditions with higher MOI (main effects of *MOI*: $F_{(4, 32)} = 258.708$, $p < 0.01$). In contrast, there was no main effect of *Torque*. There were also significant interactions *Phase* × *MOI*: [$F_{(8, 64)} = 8.990$, $p < 0.01$] and *Phase* × *Mass*: [$F_{(2, 16)} = 21.107$, $p < 0.01$] for the large external torque conditions (T_{EXT} = 0.30 Nm) but not for the small external torque (T_{EXT} = 0.22 Nm) conditions. The interactions were due to the fact that F^n_{RES} increased faster across the three phases for objects with larger mass (but not for objects with larger torque and the same mass).

The grip force (F_{GRIP}) was estimated as the sum of the absolute values of normal forces of all the digits minus F^n_{RES}. F_{GRIP} showed an increase during the handle acceleration (main effect of *Phase*: $F_{(2, 16)} > 37.612$, $p < 0.01$); it was higher for higher external torques (compare M_1L_1 and M_1L_3 in Fig. 4c; effect of *Torque*: $F_{(2, 16)} = 91.737$, $p < 0.01$), but there were no significant effects of mass (similar values for M_1L_1 and M_3L_1 in Fig. 4c). The interaction effects were significant for *Phase* × *MOI*: [$F_{(8, 64)} = 9.381$, $p < 0.01$], *Phase* × *Torque*: [$F_{(4, 32)} = 12.876$, $p < 0.01$], and *Phase* × *Mass*: [$F_{(2, 16)} = 11.250$, $p < 0.01$] for the large T_{EXT} = 0.30 Nm but not for the small T_{EXT} = 0.22 Nm. The interactions reflected the fact that the *MOI* effect on F_{GRIP} increased with *Phase*.

The resultant M^Y increased with torque (larger values for M_1L_3 as compared to M_1L_1 in Fig. 4c; main effect of *Torque*: $F_{(2, 16)} = 356.898$, $p < 0.01$). When the conditions with similar torques but different masses were compared (M_1L_3 and M_3L_1 in Fig. 4c) at T_{MAX}, M^Y showed a modest increase for the condition with the smaller mass (main effect of *Mass*: $F_{(1, 8)} > 5.458$, $p < 0.05$). M^Y increased during the acceleration phase (main effect of *Phase*: $F_{(2, 16)} > 44.776$, $p < 0.01$). The interaction effects were significant for *Phase* × *MOI*: [$F_{(8, 64)} = 19.899$, $p < 0.01$], *Phase* × *TQ*: [$F_{(4, 32)} = 25.508$, $p < 0.01$], and *Phase* × *Mass*: [$F_{(2, 16)} = 10.515$, $p < 0.01$] at large T_{EXT} = 0.30 Nm but not at small T_{EXT} = 0.22 Nm. Similar to the F_{GRIP}, the interactions reflected the fact that the *MOI* effect on M^Y increased with *Phase*.

Moment of inertia had significant main effects on all the mentioned outcome variables. However, since MOI scales with mass and lever arm, these effects could be secondary to scaling of the outcome variables with mass and external torque. To explore further the effects of MOI, Fig. 5 was arranged in an ascending MOI order (MOI values are shown in

brackets in Nm^2). Note that there was no systematic trend for any of the variables with MOI (F^n_{RES} and F_{GRIP} data are shown in Fig. 5). In particular, the M_1L_2 and M_1L_3 conditions that were associated with the largest MOI magnitudes showed a drop in F^n_{RES} and a non-monotonic change in F_{GRIP}. Pair-wise comparisons with Bonferroni corrections confirmed significant differences in F^n_{RES} among conditions with different masses (M_1L_1, M_2L_1, and M_3L_1; $p < 0.01$) but not across the three conditions with the same mass but large differences in MOI (M_1L_1 vs. M_1L_2 and M_1L_3). There were no significant differences in F_{GRIP} and M^Y (not illustrated) between conditions M_2L_1 and M_1L_2, while there were large MOI differences. In contrast, F_{GRIP} increased significantly from M_1L_1 to M_1L_2 and to M_1L_3 ($p < 0.01$).

Safety margin of the thumb

The safety margin (SM) was defined as the relative amount of additional normal force above the minimal value required to prevent slippage given the actual tangential force (see "Methods"). SM decreased in the course of handle acceleration (main effect of *Phase*: $F_{(2, 16)} > 15.507$, $p < 0.01$). It also dropped with an increase in T_{EXT} (main effect of *Torque*: $F_{(2, 16)} = 41.134$, $p < 0.01$) and *MOI* (main effect: $F_{(4, 32)} = 21.380$, $p < 0.01$). There were no effects of *Mass* and no interactions. These effects are illustrated in Fig. 6, which shows *z*-transformed SM values (SM_Z) averaged across subjects with standard error bars (the actual mean values are presented in parentheses).

Moment of force sharing

Total moment of force about the *Y*-axis (M^Y_{TOT}) was shared almost equally between the thumb (TH) and virtual finger (VF) throughout the movement; on average, the M^Y_{VF} share was slightly higher, 53.0 ± 0.6 %. Sharing of M^Y_{TOT} across the five digits was consistent across the three phases and conditions: [TH, *I*, *M*, *R*, *L*] = [47.0 ± 0.6 %, 15.6 ± 0.4 %, 14.7 ± 0.6 %, 9.8 ± 0.5 %, 14.5 ± 0.5 %]. Across all phases, conditions, and subjects, the tangential force (M^t) generated, on average, 84.8 ± 0.7 % of M^Y_{TOT}. Figure 7 illustrated the sharing pattern across digits for two force directions M^t and M^n.

Note that the lever arm of the tangential forces was constant. In contrast, the lever arm of the normal forces could change with changes in COP_X computed with respect to the handle center. COP_X average values across conditions and subjects for each digit are illustrated in Fig. 8. Note relatively large, consistent COP_X displacements for the Thumb, *M* and R fingers, while these were close to zero for the *I* and *L* fingers. There were relatively minor COP_X adjustments in the course of the handle acceleration: Only the index finger showed significant adjustments from T_0 to T_{MAX} (main effect of *Phase*, $F_{(2, 120)} = 3.725$, $p < 0.05$), but the magnitude of those adjustments was small (Fig. 8). No other effects were found.

Multi-digit synergies

Co-variation indices (ΔV) were computed for elemental variables (forces and moments of force produced by individual digits) across trials at the two assumed hierarchy levels, VF–TH and IF (see "Methods"). Figure 9 shows averaged ΔV indices across subjects for all six components of the force and moment of force vectors at both levels, VF–TH (a, b) and IF (c). The indices were predominantly positive corresponding to negative co-variation of elemental variables at both levels, that is, synergies stabilizing the performance variables. Two two-way MANOVAs on ΔV_Z (ΔV values after Fisher transformation), *Phase* × *MOI*, across all six mechanical variables were performed at the VF–TH and IF levels.

At the VF–TH level, some of the ΔV indices decreased after the lifting onset. While the ΔV indices for three force vector components and M^X showed consistently large positive values, the values for the other two moment of force components, M^Y and M^Z, dropped and even could become negative at T_{HT} and T_{MAX} (effect of *Phase*: $F_{(12, 230)} = 41.346$, $p < 0.01$). Figure. 9b shows the values of ΔV averaged across the phases in the ascending order for MOI. The ΔV values of F^X and F^Z increased (effect of *MOI*: $F_{(24, 402)} = 3.288$, $p < 0.01$), while all the other variables showed no *MOI* effects on ΔV.

At the IF level, all components, except F^Z, showed positive ΔV value for the three phases. For F^Z, ΔV was consistently negative. All the indices decreased after the lifting onset (effect of Phase: $F_{(12, 230)} = 18.519$, $p < 0.01$).

Further, we explored the relations between ΔV indices computed at the two levels of the assumed hierarchy. Figure 10 illustrates the ΔV values after Fisher transformation (ΔV_Z) for the three force components (a, c, e) and for the three moment of force components (b, d, f) at the three movement phases (T_0, T_{HT}, and T_{MAX}). Data averaged across subjects under different conditions are presented. Note the negative correlations between the ΔV_Z indices computed at the VF–TH and IF levels for the three force components over the movement phases: Higher ΔV_Z values at one level corresponded to lower ΔV_Z values at the other level. In contrast, positive correlations between the indices computed at the two levels were seen for the three moment of force variables.

Discussion

Our analysis of mechanical variables was limited to the early phase of the action, from steady state to peak acceleration. Corrective actions based on the actual movement kinematics were impossible at two of the selected instants, T_0 and T_{HT} peak F^n_{RES}, which happened at about 87 ms after the movement initiation. Such actions were also unlikely at the time of peak acceleration (T_{MAX}, 175 ms after the movement initiation), given that no perturbation happened during the movement (cf. Fishbach et al. 2007). The similarity of trends for all the outcome variables from T_0 to T_{HT} and from T_{HT} to T_{MAX} suggests that no online corrections took place and that the observed patterns reflected feed-forward control based on the perceived load before the movement initiation and memory from previous trials.

The results have confirmed our Hypothesis-1 that resultant force and resultant moment of force would scale with the corresponding external variables, load and torque, as expected from classical mechanics. This is not surprising given that the movement kinematics were highly consistent across conditions (see, for example, Fig. 3d). Note that such a consistency is not a trivial fact: The subjects were instructed to move the handle as quickly as possible; nevertheless, they scaled the applied forces and moments of force with the external load/torque to perform movements approximately within the same time. In terms of the dual-strategy hypothesis (Gottlieb et al. 1989), while the instruction was typical of the speed-insensitive strategy (Gottlieb et al. 1990), the subjects used a speed-sensitive one (Corcos et al. 1989). This result shows that behaviors during unconstrained movements may not follow the rules established for highly constrained tasks, such as those that formed the foundation of the dual-strategy hypothesis.

The lack of consistent effects of moment of inertia on the resultant moment of force may be viewed as a reflection of the fact that the subjects successfully avoided rotating the handle during the task performance. Grip force and safety margin both scaled with the external torque but not mass. These results are less trivial and will be discussed later. Safety margin showed major changes with the loading conditions and it dropped in the course of the

movements (when acceleration increased). This result refutes our Hypothesis-2 that safety margin would increase during the movement. Hypothesis-3 predicted that some of the synergy indices might not show a drop during the increase in the rate of the corresponding performance variable. Indeed, we found that several mechanical variables were strongly stabilized by multi-digit synergies and the synergy index did not drop with the rate of change of those variables. This result contradicts several previous studies (Latash et al. 2002; Friedman et al. 2009; Skm et al. 2010) on changes in the synergy index with the rate of change of the variable for which the index was computed. We also found trade-offs between synergy indices at the two levels of the assumed hierarchy for force variables only but not for moment of force variables (cf. Gorniak et al. 2009; Wu et al. 2012). Further, we discuss implications of these results for the control of a quick lifting action and multi-digit synergies.

Mechanics and control with referent configurations

While the resultant normal force changed with mass but not with external torque, the grip force changed with external torque but not with mass. Note that the grip force was computed as the internal force, that is, the sum of the absolute magnitudes of all digit forces minus the resultant. While both the resultant and the grip forces were computed from the same set of normal digit forces, the difference in their scaling with the two loading factors suggests that they were controlled as independent variables.

These observations fit the ideas of the referent configuration hypothesis (Feldman and Levin 1995). According to this hypothesis (which is a generalization of the equilibrium-point hypothesis, Feldman 1966), the neural control of actions is associated with sending control signals to groups of neurons that define a set of referent values for salient task-related coordinates (given the external force field) referred to as the referent configuration. Actual forces and displacements depend on the external loading conditions. It has been suggested (Pilon et al. 2007; Latash 2010) that the control of prehensile actions is associated with setting a magnitude of referent aperture, which results in the generation of equal and opposing grip forces because the rigid walls of the handle do not allow the digits to move toward their referent coordinates. In addition, the location of the central point of the referent aperture may be shifted resulting in net force production in one of the directions.

This mechanism of control is illustrated in Fig. 11, which shows the forces generated by two opposing digits (thumb and VF) and the location (AP_{CTR}) and size (AP_{REF}) of the referent aperture. Note that changes in AP_{CTR} produce changes in the resultant force, while changes in AP_{REF} produce changes in the grip force. The referent configuration for this component of action may be viewed as consisting of two components, AP_{REF} and AP_{CTR}. Our results suggest that the former value was adjusted to the external torque, while the latter one was adjusted to external load (mass). Note that changes in AP_{REF} produce equal changes in the referent position for the opposing digits, resulting in changes in the normal digit forces of equal magnitude. These forces play two roles, generating the moment of force by the normal forces and providing sufficient friction to generate tangential forces that were responsible for over 80 % of the total moment of force. It is not surprising, therefore, that AP_{REF} and the ensuing changes in the grip force changed with the external torque and were relatively immune to changes in the load. Changes in AP_{CTR} produced resultant normal force, which naturally correlated with load, not with torque.

The observed adjustments of the normal and tangential forces across conditions and during the three phases of the action show that the safety margin (SM) was not kept constant. It could drop by 25–30 % both across the conditions (compare M_1L_1 and M_1L_3) and across the movement phases (compare T_0 and T_{MAX} for M_1L_3). These observations speak against the hypothesis that co-adjustments of the normal and tangential forces during manipulation are

organized to keep SM constant (Johansson and Westling 1988; Burstedt et al. 1997, 1999; Cole et al. 1999; Flanagan et al. 1999; De Freitas et al. 2009). They suggest that the relation between the magnitudes of the normal and tangential forces can change to fit specific task conditions. Note that the observed drop in the safety margin in the course of the movement is counter-intuitive. Indeed, the idea of signal-dependent noise (Harris and Wolpert 1988) suggests that an increase in the applied tangential forces seen during the acceleration phase was likely associated with an increase in variance of those forces. This asks for a larger SM to ensure comparable safety of the action across all phases. The observed smaller values of SM suggest that during the movement, the system operated closer to the slippage point (see also Zatsiorsky et al. 2005).

Finger specialization in moment production

Most earlier studies with holding a vertically oriented object reported nearly equal moments of force produced by the normal and tangential digit forces (Zatsiorsky et al. 2003a, b). In a recent study (Sun et al. 2011), the share of the total moment produced by the normal forces was even higher than 50 %. In contrast, in the current study, as well as in a related study with static tasks (Wu et al. 2012), tangential forces produced over 80 % of the total moment of force. This sharing could be due to the unequal moment arms that were higher for the tangential forces and were limited for the normal forces by the small displacements of the COP of individual digits.

Several earlier studies of prehension tasks with a vertically oriented handle led to a conclusion that the middle finger pair (middle and ring fingers) was primarily involved in supporting the load, while the lateral finger pair (index and middle fingers) was primarily responsible for generating rotational action (Zatsiorsky et al. 2002, 2003b). This could be due to the fact that the lever arms for the normal forces of the *I* and *L* fingers with respect to rotation about the transverse axis of the handle (*X*-axis) were much larger than those for the *M* and *R* fingers. In contrast, in our experiment, all four fingers had equal or similar lever arms for resisting the external torque (acting about the *Y*-axis). Nevertheless, finger specialization persisted: Only the *M* and *R* fingers produced consistent moments of force with normal forces due to consistent, non-zero COP shifts. In contrast, the lateral fingers (*I* and *L*) showed a close to zero net COP shift in the *X* direction and, as a result, their normal forces produced close to zero moments. These observations suggest that finger specialization persists even when changes in the mechanical conditions do not favor it.

The sharing of the total moment between the thumb and VF and across the individual fingers did not depend on loading conditions and persisted through the three movement phases. This result suggests that the neural controller may simplify the control of the tasks by using a single default solution across conditions and phases. This solution may consist of selecting a particular direction of force vectors for the digits and scaling them with loading conditions and movement phase as needed by the task mechanics. Using such a rule for the generation of forces is compatible with the referent configuration hypothesis (see above). Indeed, shifting a referent coordinate for the tip of a digit along a straight line is associated with the generation of force vectors with proportional changes in their tangential and normal components. If this rule is applied to all digits, a standard sharing may be expected between the contributions of the normal and tangential forces to the total moment of force (assuming no changes in the lever arms—a safe assumption for our data, see Fig. 8).

Multi-digit synergies

Similar to earlier studies, we quantified prehension synergies at the two assumed hierarchical levels (VF–TH and IF) as co-variation indices of elemental variables across repetitive trials (reviewed in Latash et al. 2007; Latash and Zatsiorsky 2009). Overall, high

synergy indices confirmed that the components of the resultant force and moment of force were stabilized at both levels. One notable exception was the synergy index for the normal force quantified at the IF level: As in several earlier studies (Gorniak et al. 2009; Wu et al. 2012), we observed no synergies stabilizing the normal force produced by the VF.

Several earlier studies documented a drop in the synergy index with the rate of change of the corresponding variable. The rates of change of most variables differed significantly across the three movement phases (see Figs. 2, 3). Nevertheless, several synergy indices showed no changes across the three phases. This observation is not readily compatible with an earlier model on the origins of synergy indices during fast actions (Goodman et al. 2005). According to this model, variability in each elemental variable is defined by variance in two parameters related to the magnitude and timing of that variable. Within the model, the lack of co-variation among the timing parameters for individual elemental variables resulted in lower synergy indices at high rates of change of the performance variable (see also Latash et al. 2002). In our experiments, the expected drop in the synergy indices at the VF–TH level was seen for M^Y and M^Z only, while all the force vector components and M^X showed no decrease in the indices with movement. In contrast, at the IF level, synergy indices for all the force and moment variables dropped at T_{HT} as compared to T_0. At this time, we cannot offer an unambiguous interpretation for these contrasting results. It is possible that for some performance variables, the central nervous system is able to arrange co-variation of the timing parameters to elemental variables (cf. Latash et al. 2004) that makes variance immune to rate of change of the variables. It is also possible that another mechanism compensated for the seemingly unavoidable drop in synergy indices with speed of change of the variables.

Several earlier studies documented a trade-off between synergy indices computed at the two hierarchical levels (Gorniak et al. 2007, 2009). Indeed, using highly variable combinations of elemental variables to produce the same performance variable at the upper level leads to a very high synergy index. But the same high variability of the VF output hurts synergy index at the lower level. Studies of static prehension have shown that the trade-off is inherent to some of the variables but not to others (Gorniak et al. 2009; Wu et al. 2012). Our results confirm this conclusion for synergies associated with quick manipulation tasks. Indeed, we observed such trade-offs for force components, but not for moment of force components (Fig. 10).

The following interpretation has been offered for a similar set of results in a study with static prehension (Wu et al. 2012). For all the force variables, at the VF–TH level, the number of elemental variables was always two, while all the moment variables got contributions from both normal and tangential forces produced by each digit. Besides, lever arms of the forces could also be modified. So, the magnitudes of forces produced by the thumb and VF had to co-vary to produce force-stabilizing synergies but they might not co-vary to produce moment-stabilizing synergies. For example, such synergies could be produced by co-varied contributions of the normal and tangential forces within each digit. The availability of such a strategy allows organizing synergies at two levels within a two-level (multi-level) hierarchy that do not compete with each other but may actually show parallel changes with task conditions (see positive correlations for the moment-related synergy indices in Fig. 10). The issue of the organization of synergies within a hierarchical system has been discussed in a recent target article (Latash 2010) and associated commentaries; this issue is central in the attempts to link the idea of synergic control to the referent configuration hypothesis of motor control.

Concluding remarks

Our study has led to both predictable and unexpected results. Among the latter, we would like to reiterate the following.

First, despite the instruction to move "as quickly as possible," the subjects scaled command to the digits with the external loading condition to produce nearly identical kinematics. This result stands in stark contrast to the observations of patterns typical of the speed-insensitive strategy under similar instructions when the subjects performed constrained tasks.

Second, safety margin was not kept constant across conditions and it dropped during the action. This means that co-adjustments of the normal and tangential forces during object manipulation are task-specific and may lead to a drop in the safety cushion during the movement.

Third, the scaling of different components of the normal forces (such as the resultant and grip force) with load and torque fits well the idea of control with referent configu-rations. It suggests that different components of a referent configuration (such as those illustrated in Fig. 11) are adjusted to different characteristics of the external conditions. The data also suggest that a simple general rule may be used to adjust the action to the external conditions.

Fourth, we confirmed specialization of different fingers with respect to different task components for quick manipulation tasks. The results are similar to those reported for static prehensile tasks and suggest that finger specialization is a general feature common across a variety of tasks.

Fifth, the neural organization of multi-digit synergies in a hierarchal system shows intriguing, sometimes unpredictable, behaviors. The lack of effects of the rate of change of performance variables on synergy indices remains unexplained. The observations of the trade-off between the synergy indices computed at the two hierarchical levels for the force variables but not for the moment of force variables suggest that the degree of redundancy (the number of excess elemental variables) at the higher level of the hierarchy may allow the controller to facilitate synergies at both levels of the hierarchy.

In conclusion, we would like to emphasize the main implications of the results for theories of the neural control of movements involving redundant sets of elements. We view the referent configuration hypothesis as the only productive framework to analyze redundant (rather abundant, Latash 2012) systems. Within this hypothesis, our results suggest that components of a referent configuration may be adjusted to task mechanical characteristics using simple scaling rules thus avoiding computations (or simulations) of the numerous complex input–output relations within the human body and between the body and the environment. The referent configuration hypothesis suggests a plausible mechanism of emergence of multi-element synergies stabilizing potentially important performance variables (Latash 2010). Our results suggest that such a mechanism is able to selectively protect synergies related to stabilization of some performance variables from the seemingly unavoidable detrimental effects of the rate of change of those variables. We do not know how this is achieved, and this is potentially the most intriguing result that requires further investigation. Our results corroborate an earlier hypothesis (Wu et al. 2012) that large numbers of apparently redundant elemental variables are not the source of additional computational problems for the central nervous system but may be beneficial allowing to facilitate synergies at both levels of the hierarchy.

Acknowledgments

The study was supported in part by NIH grants AG-018751, NS-035032, and AR-048563.

References

Arbib, MA.; Iberall, T.; Lyons, D. Coordinated control programs for movements of the hand.. In: Goodwin, AW.; Darian-Smith, I., editors. Hand function and the Neocortex. Springer; Berlin: 1985. p. 111-129.

Baud-Bovy G, Soechting JF. Two virtual fingers in the control of the tripod grasp. J Neurophysiol. 2001; 86:604–615. [PubMed: 11495936]

Bernstein, NA. The co-ordination and regulation of movements. Pergamon Press; Oxford: 1967.

Burstedt MK, Edin BB, Johansson RS. Coordination of fingertip forces during human manipulation can emerge from independent neural networks controlling each engaged digit. Exp Brain Res. 1997; 117:67–79. [PubMed: 9386005]

Burstedt MK, Flanagan JR, Johansson RS. Control of grasp stability in humans under different frictional conditions during multidigit manipulation. J Neurophysiol. 1999; 82:2393–2405. [PubMed: 10561413]

Cole KJ, Rotella DL, Harper JG. Mechanisms for age-related changes of fingertip forces during precision gripping and lifting in adults. J Neurosci. 1999; 19:3238–3247. [PubMed: 10191336]

Corcos DM, Gottlieb GL, Agarwal GC. Organizing principles for single joint movements. II. A speed-sensitive strategy. J Neurophysiol. 1989; 62:358–368. [PubMed: 2769335]

De Freitas PB, Uygur M, Jaric S. Grip force adaptation in manipulation activities performed under different coating and grasping conditions. Neurosci Lett. 2009; 457:16–20. [PubMed: 19429153]

Feldman AG. Functional tuning of the nervous system with control of movement or maintenance of a steady posture. II. Controllable parameters of the muscle. Biophysics. 1966; 11:565–578.

Feldman AG, Levin MF. Positional frames of reference in motor control: their origin and use. Behav Brain Sci. 1995; 18:723–806.

Fishbach A, Roy SA, Bastianen C, Miller LE, Houk JC. Deciding when and how to correct a movement: discrete submovements as a decision making process. Exp Brain Res. 2007; 177:45–63. [PubMed: 16944111]

Flanagan JR, Burstedt MK, Johansson RS. Control of fingertip forces in multidigit manipulation. J Neurophysiol. 1999; 81:1706–1717. [PubMed: 10200206]

Friedman J, Skm V, Zatsiorsky VM, Latash ML. The sources of two components of variance: an example of multifinger cyclic force production tasks at different frequencies. Exp Brain Res. 2009; 196:263–277. [PubMed: 19468721]

Gao F, Latash ML, Zatsiorsky VM. Internal forces during object manipulation. Exp Brain Res. 2005; 165:69–83. [PubMed: 15912369]

Gelfand IM, Latash ML. On the problem of adequate language in movement science. Mot Control. 1998; 2:306–313.

Gentilucci M, Caselli L, Secchi C. Finger control in the tripod grasp. Exp Brain Res. 2003; 149:351–360. [PubMed: 12632237]

Goodman SR, Shim JK, Zatsiorsky VM, Latash ML. Motor variability within a multi-effector system: experimental and analytical studies of multi-finger production of quick force pulses. Exp Brain Res. 2005; 163:75–85. [PubMed: 15690155]

Gorniak S, Zatsiorsky VM, Latash ML. Emerging and disappearing synergies in a hierarchically controlled system. Exp Brain Res. 2007; 183:259–270. [PubMed: 17703288]

Gorniak SL, Zatsiorsky VM, Latash ML. Hierarchical control of static prehension: II. Multi-digit synergies. Exp Brain Res. 2009; 194:1–15. [PubMed: 19048236]

Gottlieb GL, Corcos DM, Agarwal GC. Strategies for the control of voluntary movements with one mechanical degree of freedom. Behav Brain Sci. 1989; 12:189–250.

Gottlieb GL, Corcos DM, Agarwal GC, Latash ML. Organizing principles for single joint movements. III: speed-insensitive strategy as a default. J Neurophysiol. 1990; 63:625–636. [PubMed: 2329365]

Harris CM, Wolpert DM. Signal-dependent noise determines motor planning. Nature. 1988; 394:780–784. [PubMed: 9723616]

Johansson RS, Westling G. Programmed and triggered actions to rapid load changes during precision grip. Exp Brain Res. 1988; 71:72–86. [PubMed: 3416959]

Latash ML. Motor synergies and the equilibrium-point hypothesis. Mot Control. 2010; 14:294–322.

Latash ML. The bliss (not the problem) of motor abundance (not redundancy). Exp Brain Res. 2012; 217:1–5. [PubMed: 22246105]

Latash ML, Zatsiorsky VM. Multi-finger prehension: control of a redundant motor system. Adv Exp Med Biol. 2009; 629:597–618. [PubMed: 19227523]

Latash ML, Scholz JF, Danion F, Schöner G. Finger coordination during discrete and oscillatory force production tasks. Exp Brain Res. 2002; 146:412–432.

Latash ML, Shim JK, Zatsiorsky VM. Is there a timing synergy during multi-finger production of quick force pulses? Exp Brain Res. 2004; 159:65–71. [PubMed: 15480588]

Latash ML, Scholz JP, Schöner G. Toward a new theory of motor synergies. Mot Control. 2007; 11:276–308.

Pataky TC, Latash ML, Zatsiorsky VM. Prehension synergies during non-vertical grasping. I. Experimental observations. Biol Cybern. 2004; 91:148–158. [PubMed: 15378373]

Pilon J-F, De Serres SJ, Feldman AG. Threshold position control of arm movement with anticipatory increase in grip force. Exp Brain Res. 2007; 181:49–67. [PubMed: 17340124]

Shim JK, Latash ML, Zatsiorsky VM. Prehension synergies in three dimensions. J Neurophysiol. 2005; 93:766–776. [PubMed: 15456799]

Skm V, Zatsiorsky VM, Latash ML. Variance components in discrete force production tasks. Exp Brain Res. 2010; 205:335–349. [PubMed: 20680251]

Sun Y, Zatsiorsky VM, Latash ML. Prehension of half-full and half-empty glasses: time and history effects on multi-digit coordination. Exp Brain Res. 2011; 209:571–585. [PubMed: 21331525]

Wu Y-H, Zatsiorsky VM, Latash ML. Static prehension of a horizontally oriented object in three dimensions. Exp Brain Res. 2012; 216:249–261. [PubMed: 22071684]

Zatsiorsky VM, Latash ML. Multi-finger prehension: an overview. J Motor Behav. 2008; 40:446–476.

Zatsiorsky VM, Gregory RW, Latash ML. Force and torque production in static multi-finger prehension: biomechanics and control. Part I. Biomechanics. Biol Cybern. 2002; 87:50–57.

Zatsiorsky VM, Gao F, Latash ML. Prehension synergies: effects of object geometry and prescribed torques. Exp Brain Res. 2003a; 148:77–87. [PubMed: 12478398]

Zatsiorsky VM, Gao F, Latash ML. Finger force vectors in multi-finger prehension. J Biomech. 2003b; 36:1745–1749. [PubMed: 14522218]

Zatsiorsky VM, Gao F, Latash ML. Motor control goes beyond physics: differential effects of gravity and inertia on finger forces during manipulation of hand-held objects. Exp Brain Res. 2005; 162:300–308. [PubMed: 15580485]

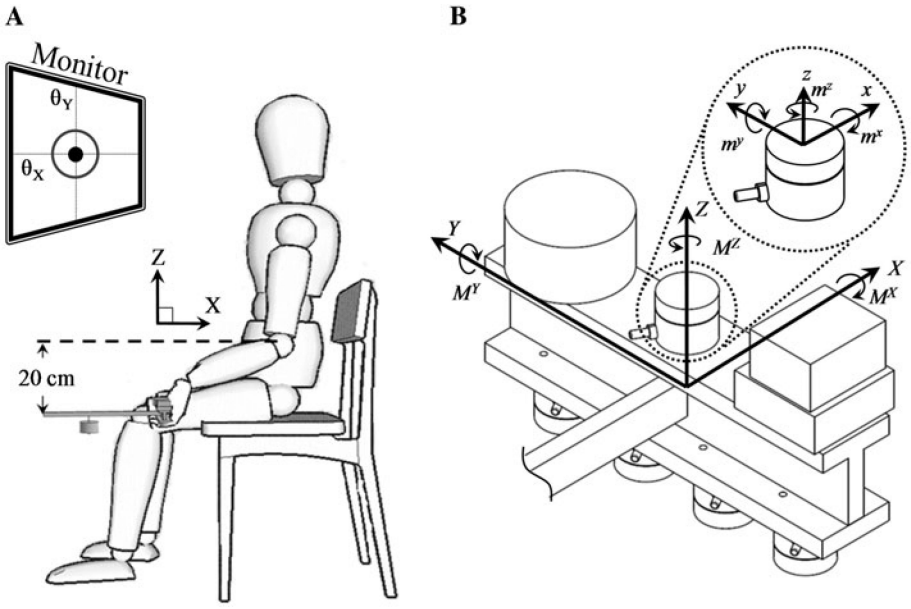

Fig. 1.

The experiment setup. **a** Position of a subject. The handle orientation feedback on the screen (θ_Y and θ_X showing the angular deviations about the *Y*- and *X*-axes, respectively, the pitch and roll angles of the handle) helped the subject maintain horizontal orientation of the handle. *b* Illustrates the local and global coordinates of the handle and sensors. For each sensor (shown as cylinders with a side connector), M^X, M^Y, and M^Z are the moment with respect to the global *X*-, *Y*-, and *Z*-axes; m^x, m^y, and m^z are the local moments with respect to local *x*-, *y*-, and *z*-axes of each sensor. The square object on the top of the handle shows the location of the sensor of the Polhemus system used for angular feedback. The cylinder on the far side of the handle represents a weight that counterbalanced the torque created by the Polhemus sensor with respect to a horizontal axis (in *X* direction) passing through the center of the thumb sensor

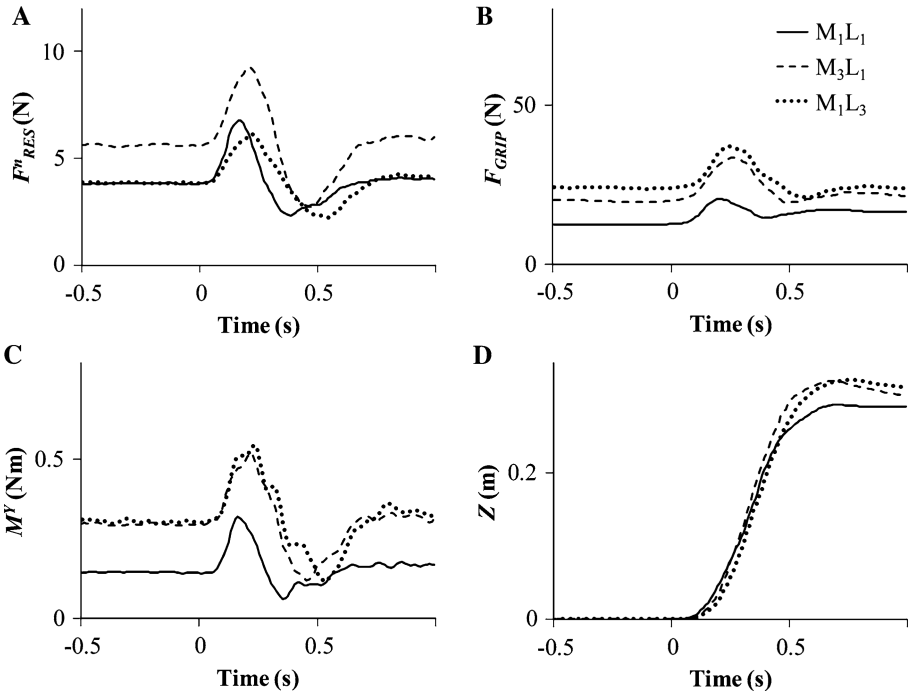

Fig. 2.

Typical behavior of a representative subject in a subset of conditions; averaged across 20 trials data are shown. **a** Resultant normal force F^n_{RES}, **b** Grip force F_{GRIP}, **c** Resultant moment M^Y, and **d** Vertical handle displacement. The *solid lines* represent the condition M_1L_1, the *dashed lines*—the condition M_3L_1, and the *dotted lines*—the condition M_1L_3

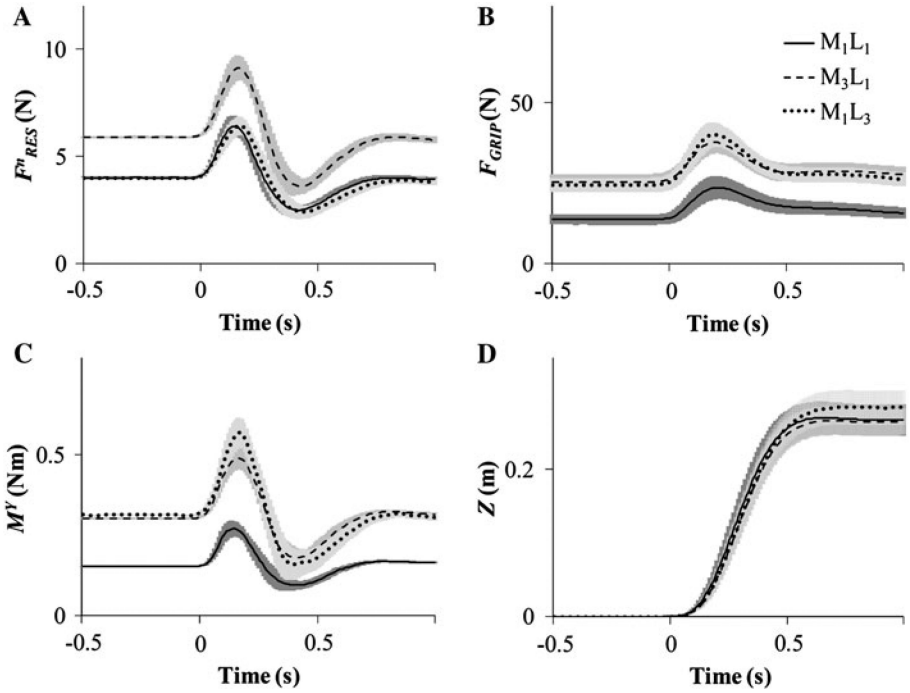

Fig. 3.

Mechanical variables averaged across subjects are shown for a subset of conditions with standard errors shown with *shades*. **a** F^n_{RES}, **b** the grip force F_{GRIP}, **c** M^Y, and **d** the vertical displacement. The solid, dashed, and dotted lines represent the conditions M_1L_1, M_3L_1, and M_1L_3, respectively

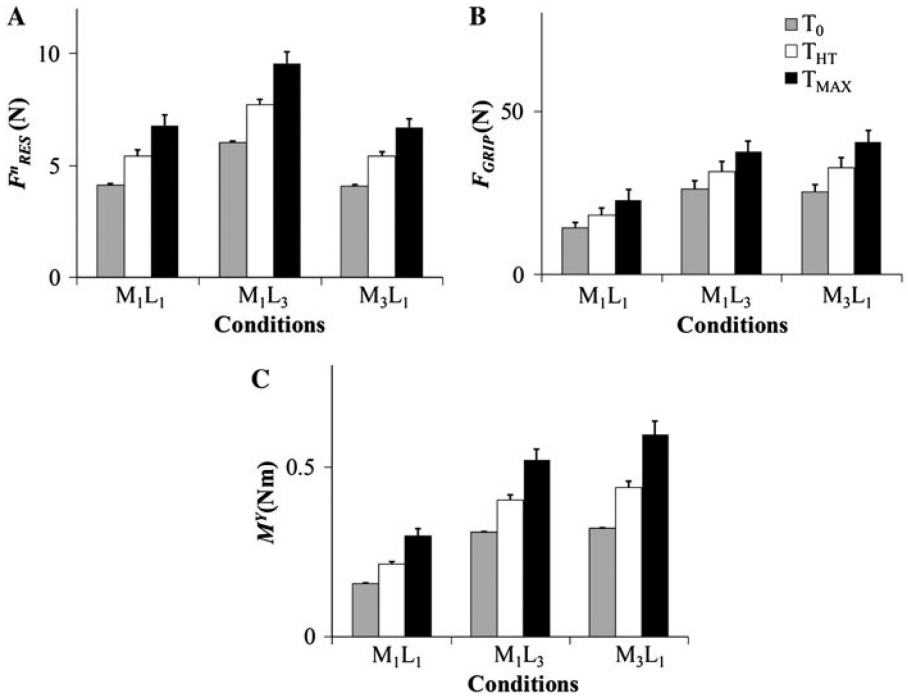

Fig. 4.

Three mechanical variables (F^n_{RES}, F_{GRIP}, and M^Y) at three lifting phases (T_0, T_{HT}, and T_{MAX}) averaged across subjects are illustrated for three conditions (M_1L_1, M_1L_3, and M_3L_1). The *error bars* represent the standard errors

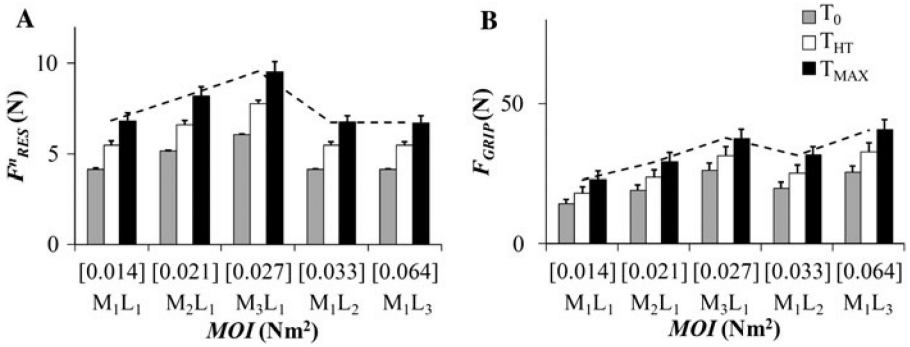

Fig. 5.

Resultant normal force, F^n_{RES} and F_{GRIP} averaged across subjects are shown for five conditions arranged in ascending MOI order. MOI values are presented in parentheses in Nm^2. None of the variables showed a systematic trend with MOI. The trends are illustrated with the *dashed lines*

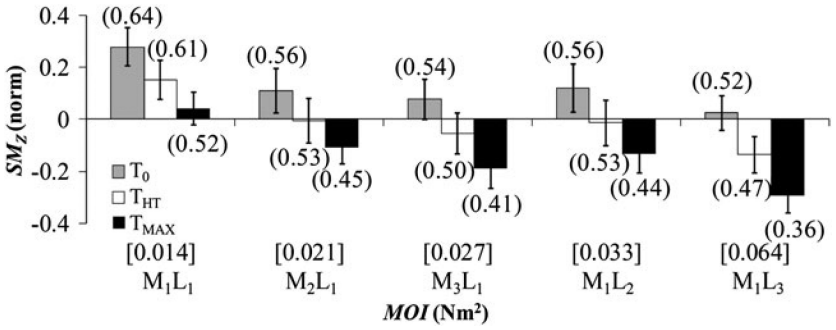

Fig. 6.

Z-transformed safety margin (SM_Z) averaged across subjects with standard error bars (actual mean SM values are shown in the *parentheses*) for the three movement phases (T_0, T_{HT}, and T_{MAX}). SM decreased during the movement and also declined with an increase in torque and MOI

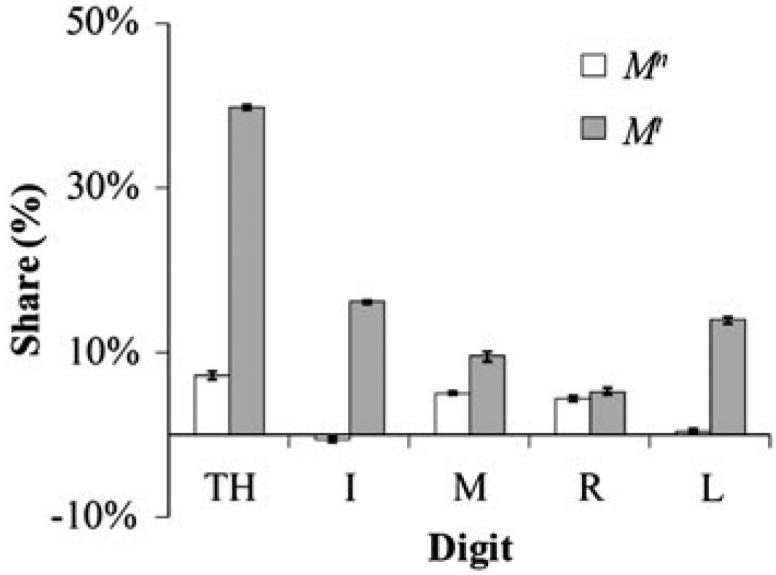

Fig. 7.

The shares of M^Y_{TOT} produced by the normal and tangential forces of the five digits. Averages across conditions and subjects are shown with standard errors. TH—thumb; *I, M, R, L*—index, middle, ring, and little fingers, respectively. Note the close to zero moments produced by the normal forces of *I* and *L*, while these fingers produced relatively large moments by their tangential forces

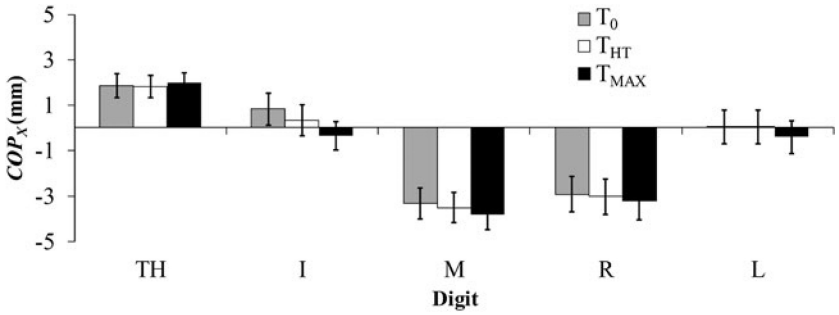

Fig. 8.

Shifts of the center of pressure (COP_X) for individual digits averaged across subjects and conditions with standard error bars are presented. During the movement, only COP_X of index finger showed small changes. Across all conditions, COP_X of only the thumb (TH), middle finger (*M*), and ring finger (*R*) was significantly different from zero, while it was about zero for the index (*I*) and little (*L*) fingers

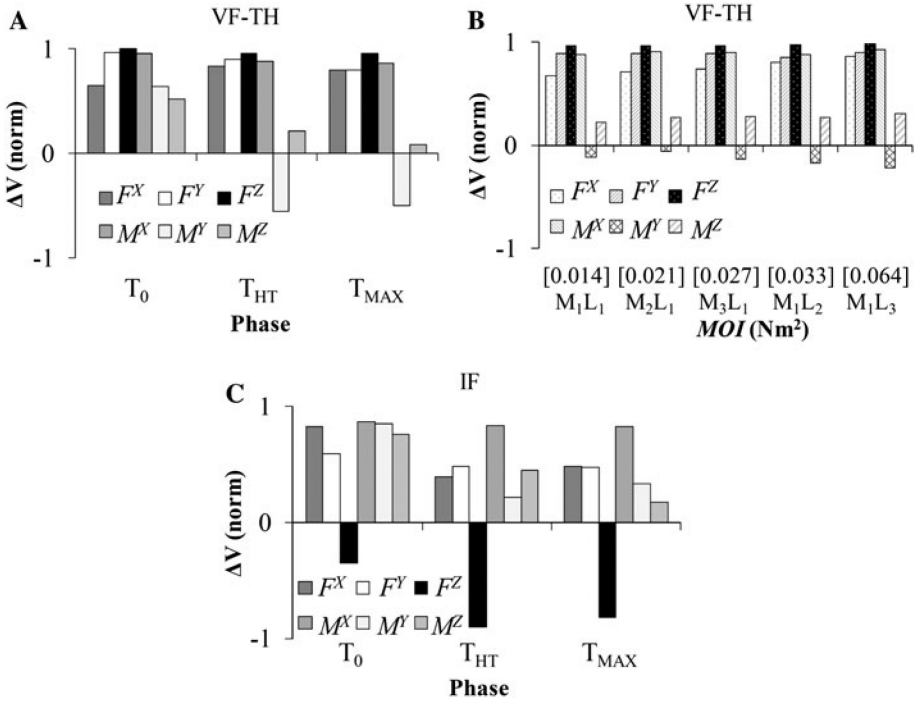

Fig. 9.

Indices of co-variation of elemental variables (ΔV) averaged across subjects for all six components of the force and moment of force vectors. **a** the values averaged across conditions at the VF–TH level; **b** the values averaged across phases at the VF–TH level. **c** the values averaged across conditions at the IF level. Note the predominantly positive values of ΔV and no changes in ΔV during the action at the VF–TH level for all the force variables

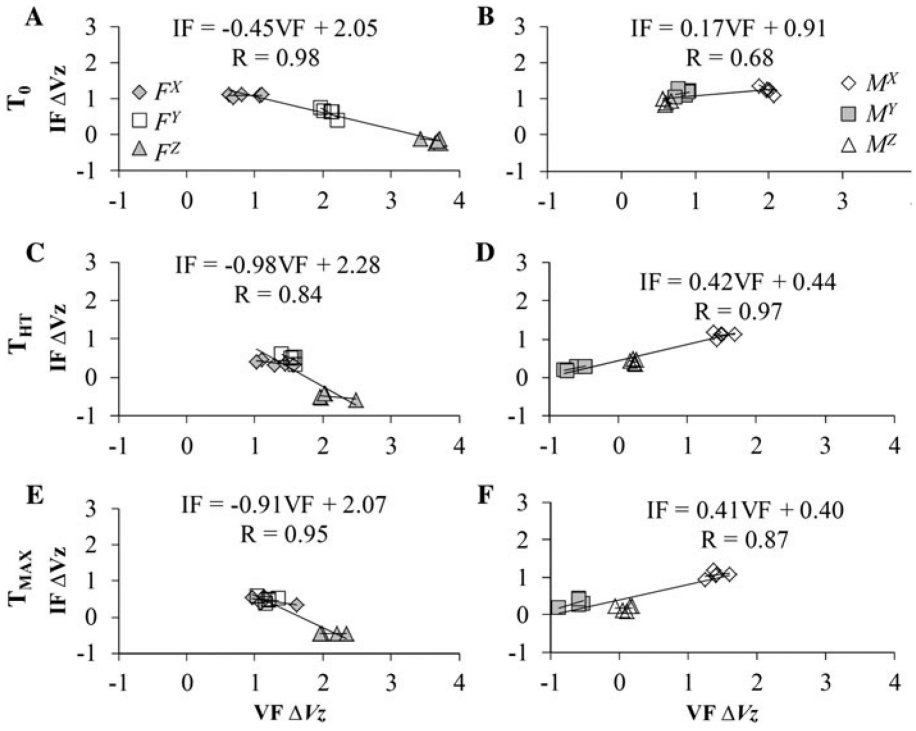

Fig. 10.

Synergy indices after Fisher's transformation (ΔV_Z) averaged across subjects and trials at the VF–TH and IF levels for the three force components (**a**, **c**, **e**) and the three moment components (**b**, **d**, **f**) at the three movement phases (T_0, T_{HT}, and T_{MAX}). Linear regression equations are shown with correlation coefficients. Note the strong negative relationships for the force variables (**a**, **c**, **e**) but positive relationships for the moment variables (**b**, **d**, **f**)

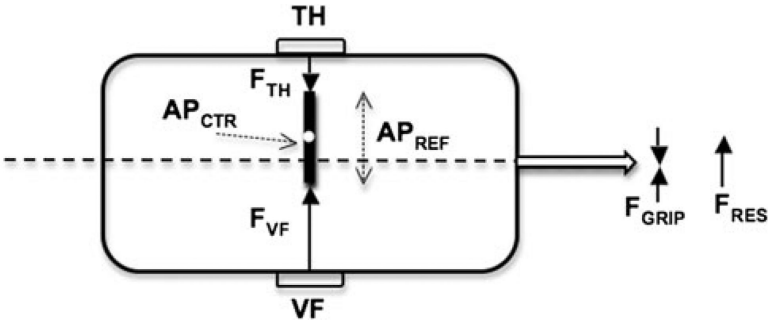

Fig. 11.

The scheme shows the results of control with referent aperture (AP_{REF}) and its central coordinate (AP_{CTR}). The distance between the actual point of force application of the thumb (TH) and virtual finger (VF) generates forces toward the referent coordinates. These result in a combination of the resultant force (F_{RES}) and grip force (F_{GRIP}) shown to the right of the drawing. The *dashed line* shows the center of the handle

Table 1

Handle deviations during movement

Deviation from steady state	At T_{HT} (Mean ± SE)	At T_{MAX} (Mean ± SE)
Pitch (about *Y*-axis)	–0.03° ± 0.01°	1.49° ± 0.18°
Roll (about *X*-axis)	–0.40° ± 0.07°	–0.93° ± 0.26°
Yaw (about *Z*-axis)	0.25° ± 0.41°	0.19° ± 0.41°
Anterio-posterior (*X*)	0.14 cm ± 0.02 cm	1.02 cm ± 0.10 cm
Medio-lateral (*Y*)	0.11 cm ± 0.01 cm	0.38 cm ± 0.04 cm

Deviations of the handle orientation and position from steady state at T_{HT} and T_{MAX} are shown (means across conditions and subjects with standard errors)